Study, Design and Development of Biocompatible Graphene-Based Piezoresistive Wearable Sensors for Human Monitoring

Fabrizio Marra, *Member, IEEE*, Adele Preziosi, Alessio Tamburrano, *Senior Member, IEEE*, Calwin J. Kundukulam, Patrizia Mancini, *Member, IEEE*, Daniela Uccelletti, and Maria Sabrina Sarto, *Fellow, IEEE*

***Abstract*—Wearable systems have become an integral part of our daily lives. Scientific research has succeeded in integrating various systems for monitoring human physiological parameters such as heart rate, respiration, sweating, and more. In this context, the proposed work focuses on the study, design, and development of an innovative wearable sensor based on graphene. The device was produced using a screen-printing ink filled with graphene nanoplatelets and it was integrated into a fabric through the transfer printing process. The graphene-filled ink was optimized with respect to the filler concentration, enabling the production of a smart textile that incorporates high-performance deformation sensors. Another innovative aspect of this study concerns the investigation of the biocompatibility of the sensor-integrated fabric through in vitro tests using human keratinocytes. Lastly, the sensor was integrated into a garment and tested in an operational environment for the monitoring of elbow joint movement. The results obtained indicate the potential to scale up the developed sensor technology, according to the specific considered application, while maintaining high sensitivity and process scalability. Furthermore, ensuring biocompatibility makes the proposed solution valuable for human monitoring using wearable devices.**

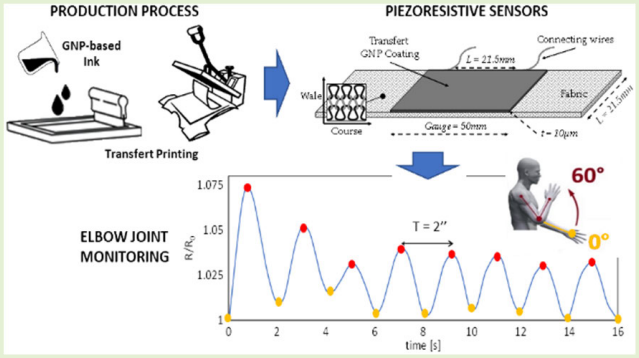

***Index Terms*— Biocompatibility, graphene, keratinocytes, real-time monitoring, smart textile, toxicity, transfer printing, wearable sensors.**

Manuscript received 17 June 2023; revised 22 September 2023; accepted 10 November 2023. Date of publication 10 January 2024; date of current version 29 February 2024. This work was supported in part by the Research Project "Digital Driven Diagnostics, Prognostics and Therapeutics for Sustainable Health Care (D34Health)," financed by Ministry of University and Research (MUR) through National Recovery and Resilience Plan (NRRP) and Piano nazionale per gli investimenti complementari (PNC) under Spoke 3, Task 3.1, which is aimed at the development, testing, and validation of innovative wearable sensor technologies for monitoring vital signs, physiological and sleep parameters, with specific reference to neurodegenerative disease, under Grant (B83C22006120001). The associate editor coordinating the review of this article and approving it for publication was Prof. Mehdi Javanmard. *(Corresponding author: Fabrizio Marra.)*

Fabrizio Marra, Alessio Tamburrano, Calwin J. Kundukulam, and Maria Sabrina Sarto are with the Department of Astronautical, Electrical and Energy Engineering and the Research Center for Nanotechnology Applied to Engineering, Sapienza University of Rome, 00185 Rome, Italy (e-mail: fabrizio.marra@uniroma1.it; alessio.tamburrano@uniroma1.it; maria.sabrina.sarto@uniroma1.it).

Adele Preziosi was with the Department of Biology and Biotechnology Charles Darwin, Sapienza University of Rome, 00185 Rome, Italy (e-mail: adele.preziosi@uniroma1.it).

Patrizia Mancini was with the Department of Experimental Medicine, Sapienza University of Rome, 00161 Rome, Italy (e-mail: patrizia.mancini@uniroma1.it).

Daniela Uccelletti is with the Department of Biology and Biotechnology Charles Darwin and the Research Center for Nanotechnology Applied to Engineering, Sapienza University of Rome, 00185 Rome, Italy (e-mail: daniela.uccelletti@uniroma1.it).

This article has supplementary downloadable material available at https://doi.org/10.1109/JSEN.2023.3336518, provided by the authors.

Digital Object Identifier 10.1109/JSEN.2023.3336518

I. Introduction

TODAY we are overwhelmed by the opportunities to utilize technology in various fields, owing to the proliferation of enabling technologies, scalable and interconnected systems, and even wearable devices [1], [2], [3]. Wearable systems have become established in a wide variety of fields such as sports, health care, and occupational safety and health [4], [5]. The sensors employed in these systems can monitor various biometric parameters, including heart rate, respiration, and perspiration, and they can also be integrated with motion sensors (accelerometer, gyroscope, and so on) [6]. Furthermore, some devices are capable of overcoming disabilities by restoring the physical and sensory functions of the person using or wearing them [7]. This technology is also on the rise due to its use in the new paradigms of the Internet of Things (IoT) for risk mitigation, by connecting heterogeneous devices to work on ever richer Big Data [8], [9].

In this context, the literature showcases the development of portable monitoring systems employing various technological solutions involving nanotechnology. Rahman and Lee [10] present recent advances in the electrochemical detection of dopamine using graphene-based sensors. These sensors demonstrate high sensitivity and selectivity, thanks to the inclusion of graphene, which possesses superior properties

for dopamine detection purposes compared to conducting polymers, carbon nanotubes, and metal oxides. Additionally, graphene is well-suited for large-scale production, making it an efficient and cost-effective material. Liu et al. [11] proposed the development of wearable carbon nanotube-based polymer electrodes for electrocardiographic measurements, employing 2-D electrodes for continuous monitoring. The wearable electrodes were fabricated by incorporating a carbon nanotube/silver-polydimethylsiloxane (CNT/Ag-PDMS) mixture into a gauze and connecting it to the measurement system using stitched wires. The proposed solution is characterized as a wearable medical device offering washable flexibility properties, making it suitable for long-term use. Furtak et al. [12] implemented a respiratory rate measurement system using sensors based on carbon nanotubes screen-printed on fabric. The limitations of this solution primarily involve optimizing the material for creating a standardized product.

In this context, the proposed work presents the study and development of a graphene-based material tailored for the design of a wearable sensor, which is versatile in geometry, shape, and biocompatible for monitoring human movement. This material was produced, optimized, and integrated into a fabric, in previous works [13], [14], using a screen printing process. In this article, we have improved the integration phase of the piezoresistive polymeric film on the fabric, through the application of a transfer printing technique, to achieve better performance and reliability of the sensorized smart textile.

Through electrical and electromechanical characterization, the percentage of graphene nanoplates (GNPs) useful for having an enhanced piezoresistive sensor response was determined. Washability tests also demonstrated the ease and flexibility of the proposed technology, as well as the possibility of long-term use. In this regard, toxicological tests of the ink filled with GNP were conducted through in vitro analysis with human keratinocytes, examining the transfer printing system based on a previous study [15].

The innovativeness with respect to the proposed literature is that in addition to the multidisciplinary characterizations that give a comprehensive view of the proposed material, the authors have studied a final application in which the system can be operational without disrupting the current working process, as suggested by routine work in the environment, health and safety (HSE).

In addition, the transfer printing technique can improve the integration between the film and fabric compared to screen printing. The versatility of the technique also allows any shape to be created and easily applied depending on the application [16].

II. Fabrication and Characterization

The manufacture of the graphene-based piezoresistive sensor was possible from the development of a screen-printed ink loaded with GNPs. The sensor design was achieved through a series of characterizations of several samples for rheology, biological compatibility, electrical conductivity, and electromechanical response tests, respectively.

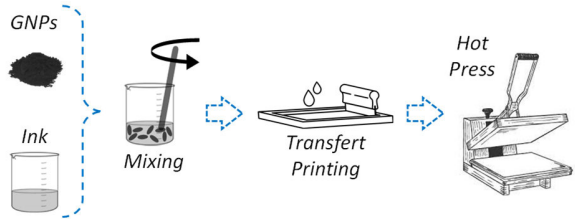

Fig. 1. Graphene-based ink and transfer printing production process.

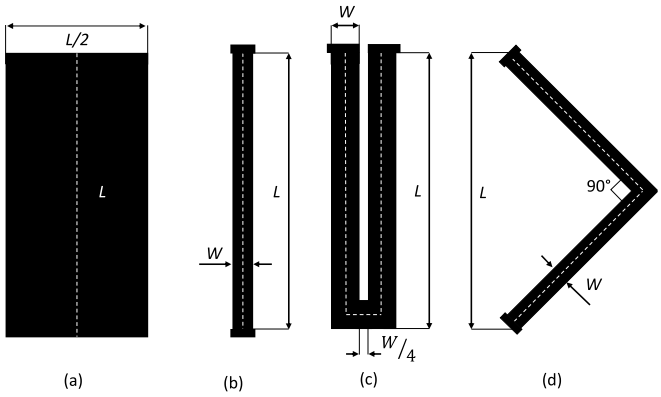

Fig. 2. Geometric representation of the piezoresistive graphene-based shapes. (a) Shape-0: Rectangular. (b) Shape 1: Single line. (c) Shape 2: U line. (d) Shape 3: Sides at 90°.

A. Graphene-Based Ink Production Process

The production process to develop the graphene-based ink started from the work [13]. It consists of two phases: the first step involves the production of GNP nanoplatelets by a thermal expansion in a muffle furnace at 1150 °C for 5 s. The by-product is exfoliated in acetone using tip sonication as described in [17]. Then, the suspension is evaporated at 90° and mixed with a water-based screen-printing ink. The second step is transfer printing, in which the previously prepared GNP-based ink is transferred on a polymetric substrate and then hot-pressed onto the fabric, as shown in Fig. 1.

The transfer-printing method employed for producing the sensors enables the creation of any shape. Different patterns were developed to investigate the sensor response as a function of its shape. Fig. 2 shows the four different shapes designed.

Shape-0 was considered as a reference shape for the preliminary tests that led to the optimization of the GNP concentration, the electrical and electromechanical characteristics of the GNP-based coatings, and the washability of the sensors.

B. Rheological Characterization

To ensure the processability and repeatability of the transfer-printing process, rheological tests were conducted to determine the ink's viscosity and optimize the sensor production process based on the filler percentage. In addition, these tests were essential to assess the quality of the dispersion of the GNPs within the matrix during the mixing step. The tests were conducted using an Anton Paar MCR302 Rheometer, at the Laboratory of Nanotechnologies and Nanosciences of Sapienza (SNN-Lab). Measurements were performed at room temperature, using a parallel plate measuring setup with a 1-mm gap and a shear rate ranging from 1 to 100 s^{-1}. The

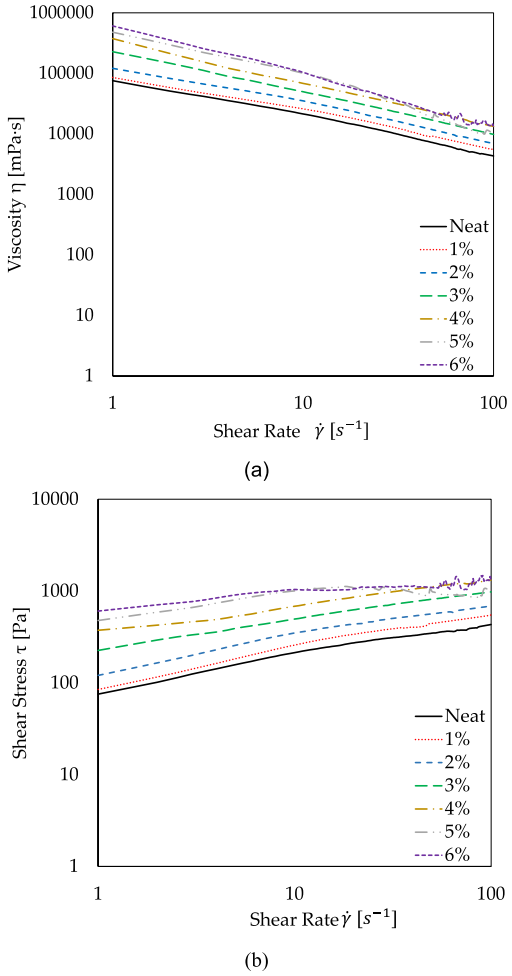

Fig. 3. (a) Viscosity measurement as a function of the shear rate. (b) Shear stress measurement as a function of the shear rate.

ink was infused with GNP concentrations ranging from 0%wt. to 6%wt. The graphs depicted in Fig. 3(a) and (b) display the viscosity and shear stress curves on a logarithmic scale as a function of the shear rate, which varies between 0 and 100 s^{-1}, also on a logarithmic scale.

The results show that conductive ink samples exhibit pseudoplastic behavior, with initial viscosities depending on the percentage of filler within the matrix, as shown in Fig. 3(a). Samples with higher concentrations of GNP show an increase in initial viscosity compared to the others, as well as a change in the slope of the curve. This trend can be explained by the presence of a GNP concentration threshold, above which the nanomaterial acts as a lubricant, leading to a decrease in the slope of the curves at high shear rates [18], [19], [20]. This behavior can guarantee good ink processability even at higher filler concentrations. From the rheological investigation, we can conclude that inks loaded with up to 6%wt. of GNP preserve viscosities that are within the workability range even at the industrial level [21], [25].

C. Biological Characterization

Biological studies were conducted at the Department of Experimental Medicine and the Department of Biology and Biotechnology Charles Darwin, Sapienza University of Rome.

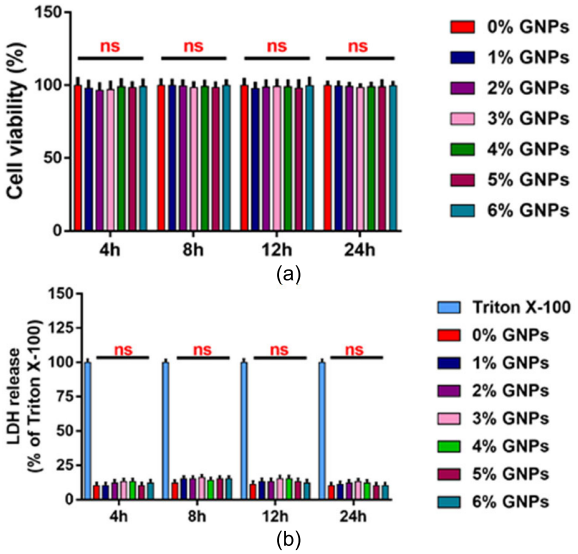

Fig. 4. Biocompatibility of patches with different concentrations of GNP on HaCaT cells. (a) MTT assay, the data are normalized to untreated patch (0%wt. GNPs) and reported as percentages. (b) LDH release, data are normalized to control treated with Triton X-100 and reported as a percentage. The values are expressed as the mean ± SD of three independent experiments. Statistical analysis was performed by the two-way ANOVA method coupled with the Bonferroni posttest (ns: not significant).

In vitro biocompatibility studies were carried out, using a human keratinocyte cell line HaCaT. Cells were cultured in Dulbecco's Modified Eagle's Medium (DMEM; Euroclone, Pero, MI, Italy), supplemented with 10% fetal bovine serum (FBS), 2 mM L-glutamine, 100 units/mL penicillin, and 100 mg/mL streptomycin (Sigma-Aldrich, MO, USA), at 37 °C with 5% CO_2 in a humidified atmosphere. Cell viability was determined using the (3- (4,5-dimethylthiazol-2-yl) -2,5-diphenyltetrazolium bromide (MTT assay), as described by Bossù et al. [22]. The fabric engineered with different concentrations of GNPs was cut into 1 × 1 cm^2 pieces, sterilized with ultraviolet (UV) light for 1 h, soaked in a culture medium, and placed over the attached cells, as previously described [15], [23]. After 4, 8, 12, and 24 h of incubation, patches were removed and the MTT assay was performed. An ELISA reader (Allsheng AMR-100 Microplate Reader, Zhejiang, China) was used to measure the absorbance at a wavelength of 570 nm and reference length of 630 nm. To determine cytotoxicity, we performed a lactate dehydrogenase (LDH) assay method, using a commercial kit (Cytotoxicity Detection kit PLUS-Hoffmann-La Roche, Basel, Swiss) according to the manufacturer's instructions. The supporting information includes the steps for the two biocompatibility tests: MTT and LHD (Figure S3 in the Supplementary Material). Each experiment was performed three times in triplicate.

Fig. 4(a) shows that HaCaT cell viability was not significantly modified after exposure to different GNP patches for all the time points considered. Even in the presence of higher concentrations of GNP, the vitality rate was very similar to the control cells. To evaluate membrane integrity, we performed an LDH assay. The level of LDH released in the culture medium during incubation with the different GNP patches remained near the value measured for the control sample and

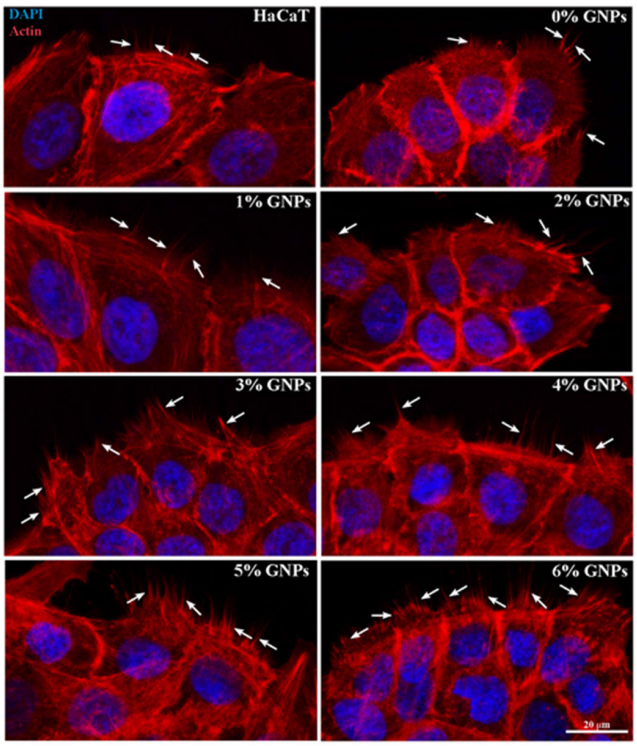

Fig. 5. Representative immunofluorescence images of HaCaT cell morphology without exposure or after exposure to different concentrations of GNP patches for 8 h. The actin cytoskeleton is highlighted by staining with TRITC-phalloidin, and the nucleus is detected by DAPI. Arrows indicate filopodia bar: 20 μm.

was not higher than 15%, in comparison to positive control (Triton X-100, taken as 100%) [Fig. 4(b)]. The statistical significance was determined by two-way analysis of variance (ANOVA) coupled with a Bonferroni posttest (GraphPad Prism 9.3.0 software, GraphPad Software Inc., La Jolla, CA, USA) and defined as $^{***}p < 0.001$ and Ns is not significant.

D. Immunofluorescence Microscopy

Immunofluorescence microscopy analysis was carried out after seeding 3×10^4 HaCaT cells on glass coverslips and left to adhere overnight. To evaluate the morphological state of the HaCaT cells, the cells were placed in direct contact with the patches with various concentrations of GNP for 8 h and were stained with phalloidin, which specifically recognizes filamentous actin cytoskeleton. The immunofluorescence was analyzed by recording stained images using an Axio Observer $Z1$ inverted microscope equipped with an ApoTome.2 System (Carl Zeiss Inc., Oberkochen, Germany). The morphological analysis showed that, under all conditions used, cells exhibited the typical polygonal morphology of keratinocytes (Fig. 5). Moreover, cells displayed the actin cytoskeleton organized mainly in filopodia, which appeared to increase in number and length as the concentration of GNP increased, as shown by the arrows in Fig. 5. So, the HaCaT cells behavior was not significantly influenced in response to the patches with different concentrations of GNP compared with the control, which is in accordance with the test.

E. Scanning Electron Microscopy

The GNP transfer-printed fabric, at different filler concentrations, was analyzed by using Zeiss Auriga Field Emission Scanning Electron Microscopy (FE-SEM), to investigate the morphology of the film and to assess its degree of integration within the textile.

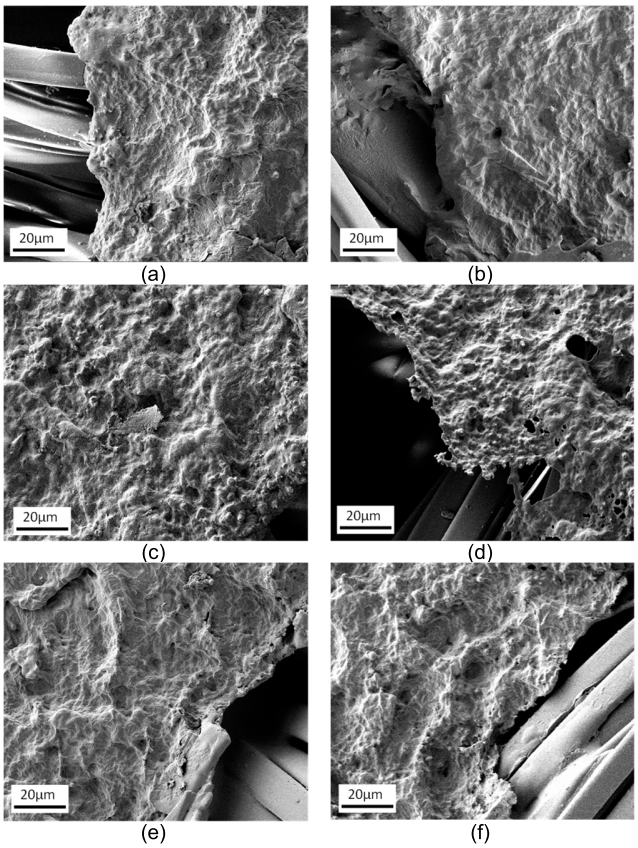

Fig. 6. Microscopy of the surface area of samples at different filler concentrations. (a) 1%wt., (b) 2%wt., (c) 3%wt., (d) 4%wt., (e) 5%wt., and (f) 6%wt. of GNP water-based ink.

To observe their surface, all samples were coated with a Cr layer approximately 20 nm thick, using a Quorum Tech Q150T sputter. Fig. 6 shows the samples of GNP-coating filled from 1%wt. to 6%wt.

From the micrographs, it was noted that the transfer printing process produces a homogeneous film with no particular morphological differences as the graphene concentration increases. In addition, this technique, unlike classical screen printing, can adhere the polymer to the substrate, providing uniform coverage and also improving the integration between film and fabric without exposing the course and wale directions. The good adhesion between the film and the textile substrate can be appreciated in Fig. 6. From the microscopy images, it can be observed that the transfer printing process reveals surface differences from the point of view of roughness; as the concentration increases, there is a change in roughness between samples with different concentrations. Furthermore, the substrate's structure is perfectly covered by the GNP films.

F. Electrical Test

The electrical characterization of the samples was conducted on samples of transfer-printed fabric (96% polyester–4% elastane) featuring a weft-knitting weave type, to determine the percolation curve as a function of GNP concentration.

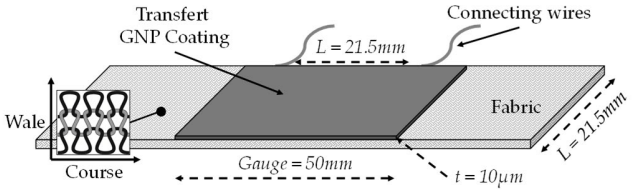

Fig. 7. Graphic representation of transfer-printed fabric samples for voltamperometric measurements and electromechanical tests.

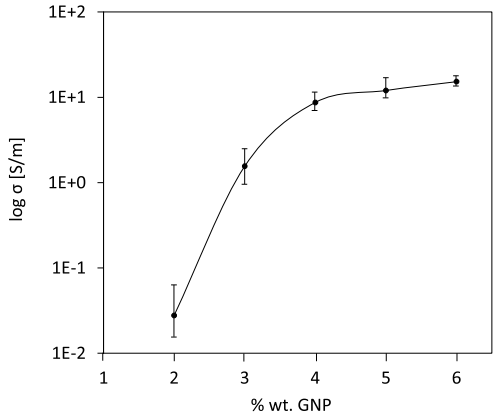

Fig. 8. Graphical representation in logarithmic scale of the conductivity for samples filled from 2%wt. to 6%wt. of GNPs.

Fig. 7 shows the geometric dimensions of the samples for the electrical and electromechanical characterizations, where L is the length of the conducting path ($L = 21.5$ mm), $t$is the thickness of the printed coating ($t = 10$ μm), and A is the area of cross section of the printed coating ($A = L \times t$). Three samples were produced for each GNP concentration, ranging from 1%wt. to 6%wt.

The resistivity (ρ) of the coatings was determined using the following formula:

$$\rho = \frac{R \times A}{L} [\Omega \text{m}] \tag{1}$$

where R represents the voltamperometric measured resistance of the specimen in ohms [Ω].

Fig. 8 shows the electrical conductivity of the coating ($\sigma = 1/\rho$). It was noticed that the 1%wt. GNP-coated samples exhibited extremely high resistance values, higher than 2%wt. GNP one within the range of megaohm, leading to their exclusion from the subsequent characterization studies.

From the conductivity graph, it can be observed that the percolation threshold is attained when the GNP concentration exceeds 1%wt. [24], [25], [26].

Electrical resistance measurements were also carried out in the sensors, with different patterns reported in Section II-A. The electrical resistance was kept constant, as much as possible, as a function of filler concentration by adjusting the size of the different Shapes 1, 2, and 3, as shown in Table I.

G. Washing Test

In addition to the aforementioned characterizations, washing tests were carried out to investigate the washability characteristics and the electrical resistance stability for samples produced with different filler concentrations.

TABLE I
GEOMETRICAL DIMENSIONS OF THE SENSORS AND THE RELATIVE ELECTRICAL RESISTANCES AS A FUNCTION OF THE GNP %

Shape	Dimensions [mm]		Resistance [Ω]				
	L	W	*2%wt. GNP*	*3%wt. GNP*	*4%wt. GNP*	*5%wt. GNP*	*6%wt. GNP*
0	50	25	$35{\cdot}10^3$	$6.4{\cdot}10^3$	$1.1{\cdot}10^1$	$0.8{\cdot}10^3$	$0.6{\cdot}10^3$
1	20	1	$10{\cdot}10^6$	$1.7{\cdot}10^5$	$2.9{\cdot}10^4$	$2.3{\cdot}10^4$	$1.7{\cdot}10^4$
2	20	2	$10{\cdot}10^6$	$1.8{\cdot}10^5$	$3.1{\cdot}10^4$	$2.4{\cdot}10^4$	$1.8{\cdot}10^4$
3	20	1.4	$9.7{\cdot}10^6$	$1.6{\cdot}10^5$	$2.8{\cdot}10^4$	$2.2{\cdot}10^4$	$1.6\ 10^4$

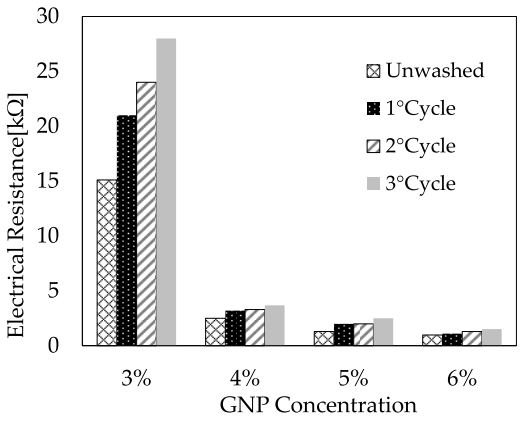

Fig. 9. Variation of electrical resistance as a function of washing cycles for the coated fabrics filled from 3%wt. to 6%wt. of GNP.

The washing test of the transfer printed fabric was performed according to the American Association of Textile Chemists and Colorists (AATCC) Test 1A Method 61-2003 [27], [28]. In this method, the fabric color loss and surface changes, if present, resulting from detergent solution and abrasive action, are evaluated through a 45-min test. The 50 × 100 mm specimens were placed in 200 mL of detergent-water solution with 0.37% detergent by volume; ten spherical beads were placed in the solution to replay the abrasive action [29]. The laundering action was generated by a magnetic stirrer with a speed of 400 r/min and a temperature controlled around 40 °C ± 2 °C. At the end of each washing cycle, a visual inspection of the washing solution was carried out to check for possible color loss. No loss in color was detected. Then, the samples were rinsed using distilled water and placed in an oven to dry at 71 °C. The electrical tests were repeated on each sample after conditioning of the sample at 65% ± 2% relative humidity at 21 °C ± 1°C for 1 h.

The stability of the electrical resistance for the different samples was studied by voltamperometric measurements before the washing test and at the end of each washing cycle. Fig. 9 presents a histogram depicting the variation of resistance values as a function of the washing cycles and GNP filler concentration.

The graph clearly shows that the initial value of the electrical resistance of the coatings increases after each wash cycle, with the most significant increase observed in the sample containing 3%wt. GNP. The mechanical effect that occurs during washing between the metal beads and the screen-printed fabric

TABLE II
STANDARD DEVIATION OF ELECTRICAL RESISTANCE AS A FUNCTION OF WASH CYCLES AND GNP CONCENTRATIONS

Electrical Resistance	GNP-based Ink			
(kΩ)	*3% wt.*	*4% wt.*	*5% wt.*	*6% wt.*
Mean Value	22.025	3.17	1.95	1.22
Standard Deviation	5.434	0.429	0.493	0.231

means that there may be mechanical stresses that affect the electrical properties of the samples. In fact, in samples with lower filler content, where there are fewer percolation paths, there is an increase in electrical resistance after each wash cycle.

Table II shows the mean values of electrical resistance and standard deviation for the measurements made on the samples at the end of the washing test; it can be seen that as the percentage increases, the standard deviation of electrical resistance decreases.

H. Electromechanical Test

The electromechanical tests were carried out following the ASTM D882 standard [30]. Quasistatic tensile tests were performed using an Instron 3366 universal machine, equipped with a 500-N load cell. The piezoresistive responses of the sensors at various filler concentrations and shapes were evaluated through measurements of the dc electrical resistance versus strain, utilizing a dc/ac current source (Keithley 6221) and a nanovoltmeter (Keithley 2182a), respectively.

The electrotechnical tests were conducted at a room temperature of 23 °C ± 3 °C, with a preload of 0.05 N; the elongations tested range from zero to 2.5% and 5%. The crosshead speed was consistently set to 2 mm/min, the current was set to $\pm 1 \times 10^{-6}$ A, and the voltage measuring range was 100 mV.

To establish an electrical connection, conductive threads were sewn onto the fabric where the GNP-based ink was transfer-printed at different filler concentrations from 3% to 6%. The gauge length is 50 mm and its width is 25 mm; different fabrics were prepared considering both the course and the wale direction of the weft-knit fabric, as shown in Fig. 7 (Section II-F). The mechanical behavior of the samples was initially investigated by examining the stress–strain variation in both course and wale directions for the pure uncoated fabric [13], [31]. Subsequently, these behaviors were compared to those of fabrics with the neat ink applied, as shown in Fig. 10. It can be noted that the values of the stress for the uncoated fabric, in this deformation range, are not appreciable with respect to the neat coated. This behavior is confirmed in both the wale and course directions of the weft-knit sample [32], [33].

Once the mechanical response of the fabric was characterized, transfer-printed fabric samples with Shape-0, at concentrations from 3%wt. to 6%wt. of GNP, were analyzed to determine their piezoresistive response.

A conditioning test was carried out to stabilize the electromechanical response. This was achieved by performing four tests consisting of three trials each; the fourth and final test was carried out after a 1-h break. Test I, Test III, and Test IV

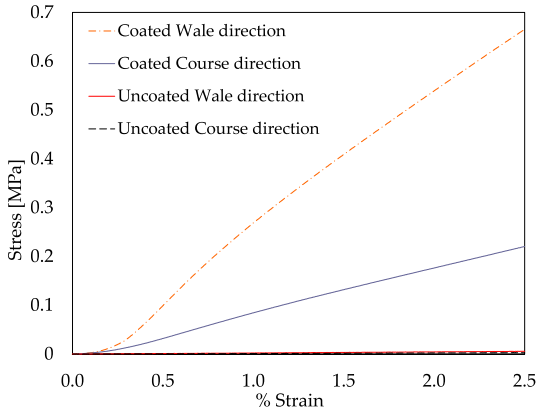

Fig. 10. Comparison of stress–strain curves for neat ink-coated and uncoated fabrics along the wale and course directions.

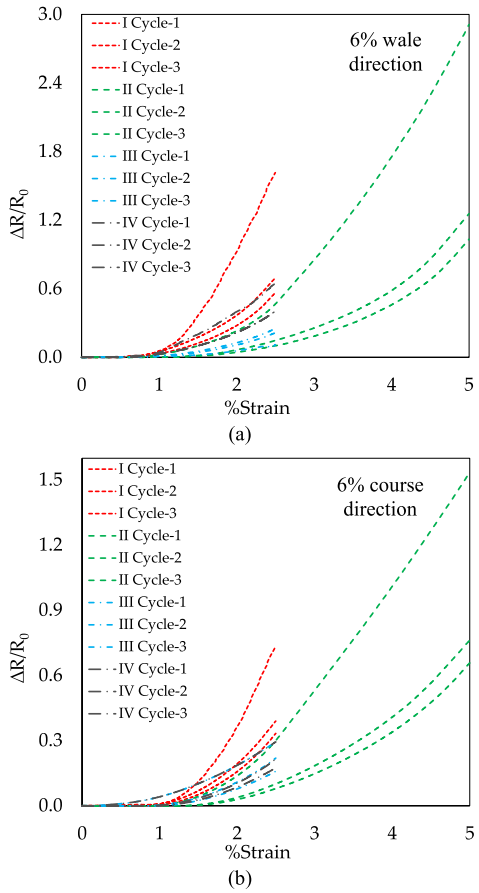

Fig. 11. Shape-0 electromechanical test at 2.5% and 5% strain for samples filled with 6%wt. of GNPs. (a) Wale direction. (b) Course direction.

were carried out with a maximum strain of 2.5%, while Test II was performed with a maximum strain of 5% for mechanical conditioning of the material.

In Fig. 11, the electromechanical test for Shape-0 transfer printed fabric at 6%wt. of GNP before the washing (unwashed) test is shown. Graphs of the samples at the different concentrations, before and after the washing step, have been included in the supporting information.

Table III shows the mean value and standard deviation of $\Delta R/R0$ at the maximum strain of 2.5%, related to the

TABLE III
MEAN VALUE AND STANDARD DEVIATION OF $\Delta R/R0$ AT MAXIMUM STRAIN 2.5% AS A FUNCTION OF SHAPE-0 GRAPHENE-BASED FABRIC AT DIFFERENT CONCENTRATIONS BEFORE WASHING TEST IN THE COURSE AND WALE DIRECTIONS

UNWASHED "SHAPE-0" $\Delta R/R_0$					
	Sample	Course direction		Wale direction	
		Mean Value	StD	Mean Value	StD
3%	As prepared	0.74	0.33	1.73	1.21
	Conditioned	0.38	0.02	0.73	0.08
4%	As prepared	0.95	0.57	1.03	0.33
	Conditioned	0.48	0.14	0.50	0.04
5%	As prepared	0.94	0.44	0.23	0.14
	Conditioned	0.42	0.06	0.20	0.12
6%	As prepared	0.48	0.22	0.55	0.15
	Conditioned	0.24	0.05	0.19	0.01

TABLE IV
MEAN VALUE AND STANDARD DEVIATION OF $\Delta R/R0$ AT MAXIMUM STRAIN 2.5% AS A FUNCTION OF SHAPE-0 GRAPHENE-BASED FABRIC AT DIFFERENT CONCENTRATIONS AFTER WASHING TEST IN THE COURSE AND WALE DIRECTIONS

WASHED "SHAPE-0" $\Delta R/R_0$					
	Sample	Course direction		Wale direction	
		Mean Value	StD	Mean Value	StD
3%	As prepared	0.88	0.39	1.23	0.74
	Conditioned	0.42	0.08	0.44	0.01
4%	As prepared	0.32	0.14	0.81	0.49
	Conditioned	0.18	0.03	0.36	0.04
5%	As prepared	0.41	0.19	0.59	0.28
	Conditioned	0.20	0.04	0.29	0.02
6%	As prepared	0.27	0.04	0.28	0.14
	Conditioned	0.12	0.01	0.15	0.02

electromechanical tests for the samples before conditioning (Test I) and for the conditioned sample (Test IV).

From the numerical values of the electromechanical test, before proceeding with the washing test, it can be seen that for all sample conditioning, it is useful to reduce the uncertainty in the measurement. At the end of the test, the response of the 6% sample has a lower standard deviation, than the other percentages, in both course and wale directions.

Electromechanical tests on Shape-0 samples were also repeated after the washing test, as described in Section II-G. The numerical values are given in Table IV.

The conditioning process leads to a reduction in the standard deviation values. This supports the assumption about the stabilization of the electromechanical response of the sensors. From the electromechanical, the samples in the wale direction have higher $\Delta R/R_0$ values to make it preferable as a final sensor than the sensor in the course direction [34], [35].

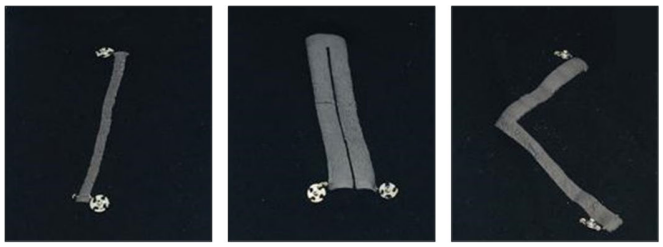

Fig. 12. Sensors for elbow joint monitoring transferred to fabric with the corresponding electrical contacts, respectively, with different shapes.

TABLE V
GEOMETRICAL DIMENSIONS AND ELECTRICAL RESISTANCES OF THE SENSORS FOR ARM FLEXION AND EXTENSION WITH DIFFERENT GEOMETRIES

Shape	Dimensions [mm]		Resistance [Ω]
	L	*W*	*6%wt. GNP*
1	80	4	$1.98 \cdot 10^4$
2	80	8	$1.93 \cdot 10^4$
3	80	5.6	$1.78 \cdot 10^4$

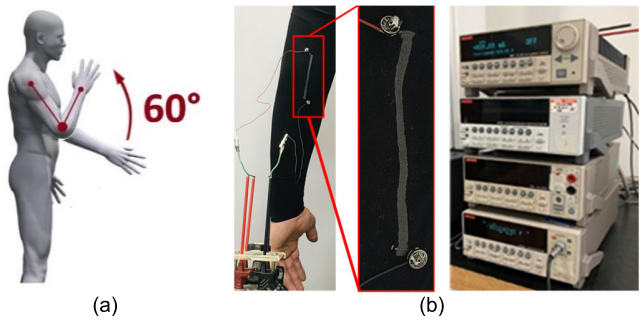

(a) (b)

Fig. 13. (a) Diagram of a single elbow flexion-extension movement. (b) Setup.

III. SENSORS FOR ARM FLEXION AND EXTENSION

Once the material and sensing device characterizations were completed, to monitor flexion-extension movements of the elbow, which may be associated with musculoskeletal problems of the elbow joint and thus with occupational hazards [14], an ink containing 6% GNP by weight was transfer printed onto an elastic sleeve (Fig. 12).

The aim was to maximize the piezoresistive response of the sensors in relation to elbow flexion-extension movement. To be able to measure the movement it was necessary to scale the dimensions of the sensors comparable with the dimensions of the elbow while keeping the electrical resistance values unchanged. At this stage, regarding the final dimensions of the sensor, it was decided not to test Shape-0. The dimensions of the sensors for monitoring the arm flexion-extension movements are shown in Table V.

The dc/ac current source and the nanovoltmeter were connected to the sensor, enabling the detection of electrical resistance changes in response to elbow joint movement routines; two metal snaps connected in turn with conductive wires were sewn to the ends of the sensors for connection to the measuring device [Fig. 13(b)].

The test consists of eight flexor extensions of the elbow at a 60° angle performed continuously [Fig. 13(a)]. The period (T)

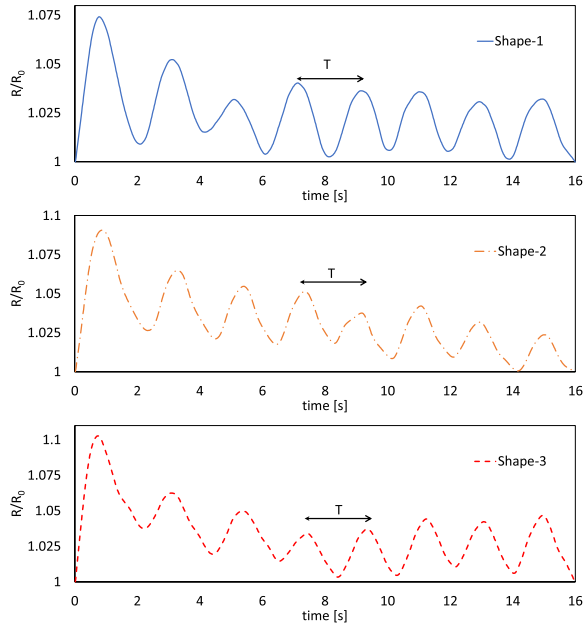

Fig. 14. Comparison of electrical resistance during elbow joint movement with a period of 2 s, for the different shapes as a function of time.

for the single flexion extension was around 2 s. The test was carried out by an operator, using conscious and nonautomated movement, with a degree of uncertainty of ≈0.2 s.

As can be seen from the real-time results in Fig. 14, the sensors can detect the movement associated with the flexion extension of the elbow. The R/R_0 data shows that the response of the three sensors is almost superimposable, except for a delay due to the manual movement of the operator.

IV. Discussion and Conclusion

The proposed work demonstrates the potential for fabricating sensors useful in monitoring elbow movement by utilizing piezoresistive patches made of graphene nanoplatelet transfer-printing coating, integrated on a fabric.

The transfer-printing technology has proven to be a solution for producing wearable piezoresistive with high sensitivity and stability. The sensors are easy to integrate, with scalable shapes depending on the physiological parameter to be monitored.

Furthermore, the rheological, electrical, and electromechanical characterizations were crucial in determining the filler concentrations suitable for the final application and the repeatability. Additionally, the washability tests demonstrated a high degree of electrical stability for the sensors after multiple washing cycles.

The biocompatibility of wearable sensors showed a high range of viability when compared to the control sample, also in line with data from previous works [15], [36]. In agreement with viability results, no damage in cell membrane integrity was observed in all conditions tested. Low GNP concentrations are not toxic to the HaCaT cell line, as already demonstrated by Salesa et al. [37]. The analysis of the cytoskeletal actin showed in all cases examined cells with a polygonal shape and an increase of filopodia at higher concentrations of GNPs, probably utilized by the cells as probes of the surrounding environment as suggested also in the case of GNP decorated with zinc oxide nanorods [38].

The geometries were designed to analyze the piezoelectric response of the fabric without knowing the pattern and orientation of the garment threads. Three geometries have distinct mechanical deformation characteristics; in fact, Shapes 1 and 2 have only one preferential direction, while Shape 3, due to its design, has a piezoresistive response in both course and wale directions.

In conclusion, the designed sensor has demonstrated that it meets the requirements of sensitivity, flexibility, lightweight, excellent washability, biocompatibility, and ease of reproducibility.

References

[1] G. Udovicic, A. Topic, and M. Russo, "Wearable technologies for smart environments: A review with emphasis on BCI," in *Proc. 24th Int. Conf. Softw., Telecommun. Comput. Netw. (SoftCOM)*, Sep. 2016, pp. 1–9.

[2] E. L. van den Broek, "Monitoring technology: The 21st century pursuit of well-being?" Eur. Agency Saf. Health Work (EU-OSHA), EU-OSHA Discuss. Pap., Spain, Tech. Rep., 2017.

[3] A. Lmberis and A. Dittmar, "Advanced wearable health systems and applications–Research and development efforts in the European union," *IEEE Eng. Med. Biol. Mag.*, vol. 26, no. 3, pp. 29–33, May 2007.

[4] J. G. Argañarás, Y. T. Wong, R. Begg, and N. C. Karmakar, "State-of-the-art wearable sensors and possibilities for radar in fall prevention," *Sensors*, vol. 21, no. 20, p. 6836, Oct. 2021.

[5] S. Seneviratne et al., "A survey of wearable devices and challenges," *IEEE Commun. Surveys Tuts.*, vol. 19, no. 4, pp. 2573–2620, 4th Quart., 2017.

[6] M. Serbanescu, V. M. Placinta, O. E. Hutanu, and C. Ravariu, "Smart, low power, wearable multi-sensor data acquisition system for environmental monitoring," in *Proc. 10th Int. Symp. Adv. Topics Electr. Eng. (ATEE)*, Mar. 2017, pp. 118–123.

[7] L. Rum et al., "Wearable sensors in sports for persons with disability: A systematic review," *Sensors*, vol. 21, no. 5, p. 1858, Mar. 2021.

[8] T. Poongodi, R. Krishnamurthi, R. Indrakumari, P. Suresh, and B. Balusamy, "Wearable devices and IoT," in *A Handbook of Internet of Things in Biomedical and Cyber Physical System*, V. E. Balas, V. K. Solanki, R. Kumar, and M. A. R. Ahad, Eds. Cham, Switzerland: Springer, 2020, pp. 245–273.

[9] W. Huifeng, S. N. Kadry, and E. D. Raj, "Continuous health monitoring of sportsperson using IoT devices based wearable technology," *Comput. Commun.*, vol. 160, pp. 588–595, Jul. 2020.

[10] M. M. Rahman and J.-J. Lee, "Electrochemical dopamine sensors based on graphene," *J. Electrochem. Sci. Technol*, vol. 10, no. 2, pp. 185–195, Jun. 2019.

[11] B. Liu, H. Tang, Z. Luo, W. Zhang, Q. Tu, and X. Jin, "Wearable carbon nanotubes-based polymer electrodes for ambulatory electrocardiographic measurements," *Sens. Actuators A, Phys.*, vol. 265, pp. 79–85, Oct. 2017.

[12] N. Furtak, E. Skrzetuska, and I. Krucińska, "Development of screen-printed breathing rate sensors," *Fibres Text. East. Eur.*, vol. 21, pp. 84–88, Nov. 2013.

[13] F. Marra, S. Minutillo, A. Tamburrano, and M. S. Sarto, "Production and characterization of graphene nanoplatelet-based ink for smart textile strain sensors via screen printing technique," *Mater. Des.*, vol. 198, Jan. 2021, Art. no. 109306.

[14] H. C. Bidsorkhi, F. Marra, A. G. D'Aloia, A. Tamburrano, G. De Bellis, and M. S. Sarto, "Piezoresistive fabric produced through PVDF-graphene nanocomposite film incorporation in textile via screen printing technique," in *Proc. IEEE SENSORS*, Oct. 2019, pp. 1–4.

[15] C. Fanizza et al., "In vitro and in vivo biocompatibility studies on engineered fabric with graphene nanoplatelets," *Nanomaterials*, vol. 12, no. 9, p. 1405, Apr. 2022.

[16] L. De Filippo, M. A. Gogliettino, and E. Guerrera, "Schede di rischio da sovraccarico biomeccanico degli arti superiori nei comparti della piccola industria," Istituto Nazionale Assicurazione contro gli Infortuni sul Lavoro (INAIL) Italy, Tech. Rep., 2014.

[17] M. S. Sarto, A. G. D'Aloia, A. Tamburrano, and G. De Bellis, "Synthesis, modeling, and experimental characterization of graphite nanoplatelet-based composites for EMC applications," *IEEE Trans. Electromagn. Compat.*, vol. 54, no. 1, pp. 17–27, Feb. 2012.

[18] D. B. Genovese, "Shear rheology of hard-sphere, dispersed, and aggregated suspensions, and filler-matrix composites," *Adv. Colloid Interface Sci.*, vols. 171–172, pp. 1–16, Mar. 2012.

[19] T. Mezger, *The Rheology Handbook: For Users of Rotational and Oscillatory Rheometers*. Hannover, Germany: Vincentz Network, 2020. [Online]. Available: https://doi.org/10.1515/9783748603702
[20] J. Lin, L. Wang, and G. Chen, "Modification of graphene platelets and their tribological properties as a lubricant additive," *Tribol. Lett.*, vol. 41, no. 1, pp. 209–215, Jan. 2011.
[21] C. Xu and N. Willenbacher, "How rheological properties affect fine-line screen printing of pastes: A combined rheological and high-speed video imaging study," *J. Coatings Technol. Res.*, vol. 15, no. 6, pp. 1401–1412, Nov. 2018.
[22] M. Bossu et al., "Biocompatibility and antibiofilm properties of calcium silicate-based cements: An in vitro evaluation and report of two clinical cases," *Biology*, vol. 10, no. 6, p. 470, May 2021.
[23] M. S. Stan et al., "Designing cotton fibers impregnated with photocatalytic graphene oxide/fe, N-doped TiO_2 particles as prospective industrial self-cleaning and biocompatible textiles," *Mater. Sci. Eng., C*, vol. 94, pp. 318–332, Jan. 2019.
[24] C.-W. Nan, Y. Shen, and J. Ma, "Physical properties of composites near percolation," *Annu. Rev. Mater. Res.*, vol. 40, no. 1, pp. 131–151, Jun. 2010.
[25] J. K. W. Sandler, J. E. Kirk, I. A. Kinloch, M. S. P. Shaffer, and A. H. Windle, "Ultra-low electrical percolation threshold in carbon-nanotube-epoxy composites," *Polymer*, vol. 44, no. 19, pp. 5893–5899, Sep. 2003.
[26] H.-J. Choi, M. S. Kim, D. Ahn, S. Y. Yeo, and S. Lee, "Electrical percolation threshold of carbon black in a polymer matrix and its application to antistatic fibre," *Sci. Rep.*, vol. 9, no. 1, p. 6338, Apr. 2019.
[27] *AATCC TM61-2013e2, Metodo Di Prova Per la Soliditá Del Colore Al Lavaggio: Accelerato*, Amer. Assoc. Textile Chemists Colorists (AATCC), Triangle Park, NC, USA, Jan. 2013.
[28] G. Cai, M. Yang, Z. Xu, J. Liu, B. Tang, and X. Wang, "Flexible and wearable strain sensing fabrics," *Chem. Eng. J.*, vol. 325, pp. 396–403, Oct. 2017.
[29] X. Tao, V. Koncar, T.-H. Huang, C.-L. Shen, Y.-C. Ko, and G.-T. Jou, "How to make reliable, washable, and wearable textronic devices," *Sensors*, vol. 17, no. 4, p. 673, Mar. 2017.
[30] *Standard Test Methods for Tensile Properties of thin Plastic Sheeting, Method D882-10*, Standard ASTM D-882, pp. 1–10, 2017.
[31] K. H. Leong, S. Ramakrishna, Z. M. Huang, and G. A. Bibo, "The potential of knitting for engineering composites—A review," *Compos. A, Appl. Sci. Manuf.*, vol. 31, no. 3, pp. 197–220, Mar. 2000.
[32] D. Mikučioniene, R. Ciukas, and A. Mickevičiene, "The influence of knitting structure on mechanical properties of weft knitted fabrics," *Medziagotyra*, vol. 16, no. 3, pp. 221–225, 2010.
[33] M. de Araújo, R. Fangueiro, and H. Hong, "Modelling and simulation of the mechanical behaviour of weft-knitted fabrics for technical applications: Part III: 2D hexagonal FEA model with non-linear truss elements," *Autex Res. J.*, vol. 4, no. 1, pp. 25–32, 2004.
[34] S. Varnaite and J. Katunskis, "Influence of washing on the electric charge decay of fabrics with conductive yarns," *Fibres Text. East. Eur.*, vol. 76, no. 5, pp. 69–75, 2009.
[35] L. Nilsson, M. Satomi, A. Vallgårda, and L. Worbin, "Understanding the complexity of designing dynamic textile patterns," in *Proc. Ambience, Art, Technology Design Meet*, Borås, Sweden, Nov. 2011, pp. 28–30.
[36] M. Stan et al., "Photocatalytic, antimicrobial and biocompatibility features of cotton knit coated with Fe-N-doped titanium dioxide nanoparticles," *Materials*, vol. 9, no. 9, p. 789, Sep. 2016.
[37] B. Salesa, A. Tuñón-Molina, A. Cano-Vicent, M. Assis, J. Andrés, and Á. Serrano-Aroca, "Graphene nanoplatelets: In vivo and in vitro toxicity, cell proliferative activity, and cell gene expression," *Appl. Sci.*, vol. 12, no. 2, p. 720, Jan. 2022.
[38] G. Ficociello et al., "Anti-candidal activity and in vitro cytotoxicity assessment of graphene nanoplatelets decorated with zinc oxide nanorods," *Nanomaterials*, vol. 8, no. 10, p. 752, Sep. 2018.

Fabrizio Marra (Member, IEEE) received the bachelor's degree in computer engineering the master's degree in nanotechnology engineering and the Ph.D. in engineering of materials, technologies and complex industrial systems from Sapienza University of Rome, Rome, Italy.

During his master's degree, he participated in the Erasmus project for a total period of seven months at the Aalto University of Helsinki, Espoo, Finland. During his Ph.D. degree, he was a Visiting Researcher with the Institute of Science and Technology of Polymers (CSIC-ICTP), Madrid, Spain. During the master's thesis and the Ph.D. thesis, he develops electromagnetic interference (EMI) screens and RAM materials, on carbon nanostructures and related polymer matrix nanocomposites, with controlled electrical and electromagnetic (EM) properties. He is with the Department of Astronautical, Electrical and Energy Engineering and CNIS, Sapienza University of Rome. His scientific activity is mainly aimed at the development and manufacture of composite materials and structures for applications in the fields of electromagnetic compatibility, sensors, and nanotechnology. In particular, the research activities are focused on the modeling, design, and production of nanostructured and multifunctional materials for EMI applications, wearable devices, and sensors for structural monitoring routines. Such research activity has led to the publication of more than 20 articles in international journals and proceedings of international symposia. His scientific production includes a chapter contribution to a book. He has coauthored one Italian patent (internationalized) in collaboration with Leonardo S.p.A. Aircraft Division–Electronics Division Turin Caselle (TO), Italy, describing the design of innovative multilayer radar-absorbing laminate.

Adele Preziosi received the Laurea degree in biotechnology and genomic for industry and environment and the Ph.D. degree in cellular and developmental biology from the Sapienza University of Rome, Rome, Italy, in 2019 and 2023, respectively.

Her scientific activity was focused on in vitro study of the effects of graphene-based nanomaterials on cultured cells and on the use of *C. elegans* as a model system. Her scientific activity is documented by seven publications in international journals.

Alessio Tamburrano (Senior Member, IEEE) received the Laurea (summa cum laude) degree in electrical engineering, the master's degree in electromagnetic compatibility and environmental impact of electromagnetic fields, and the Ph.D. degree in electrical engineering from the Sapienza University of Rome, Rome, Italy, in 2003, 2005, and 2007, respectively.

In 2022, he was appointed as a Full Professor of Electrotechnics with the Sapienza University of Rome, where he is currently with the Department of Astronautical, Electrical and Energy Engineering (DIAEE) and a Steering Committee Member with the Research Center on Nanotechnology applied to Engineering of Sapienza (CNIS). From 2010 to 2014, he was the Project Leader of the Joint Project Team 80004-9—Nanotechnologies—Vocabulary—Part 9: Electrotechnical Products and Systems of the International Electrotechnical Commission (IEC). His research activity has led to the publication of more than 100 articles in international journals and proceedings of international symposia. He has coauthored ten patents. His scientific production includes two chapters' contributions to books. His current research interests include modeling, design, and experimental characterization of nanostructured and multifunctional materials for electromagnetic applications; development of graphene-based highly sensitive piezoresistive paints/coatings and porous nanocomposites with strain sensing capabilities for structural health monitoring and wearable electronics applications; and modeling and simulation of the transmission-line performances and signal integrity of nanointerconnects made of single-wall carbon nanotube bundles, multiwall carbon nanotubes, and graphene nanoribbons for future high-speed electronics.

Prof. Tamburrano has been a member of the Working Group P 2715—IEEE guides for the characterization of the shielding effectiveness of planar materials since 2016. He received several awards from IEEE. From 2013 to 2017, he served as the Chair of the Technical Committee of the IEEE EMC Society TC-11 "Nanotechnology and Advanced Materials."

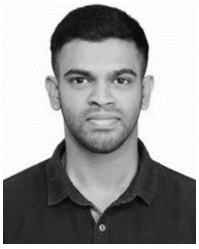

Calwin J. Kundukulam received the master's degree in nanotechnology engineering from the Sapienza University of Rome, Rome, Italy, in 2021, where he honed his skills in design, analysis, and production.

During his final thesis under the supervision of Prof. Alessio Tamburrano and Dr. Fabrizio Marra, he closely worked with wearable sensors by heat-transfer printing. In his current role as a System Performance Engineer with ASML, The Netherlands, a leading manufacturer of chip-making machines, he is responsible for calibrating the lithography systems, after they are fully assembled focusing on quality, teamwork, and communication. He is a progress-driven skilled engineer with a passion for using technology to improve people's lives.

Patrizia Mancini (Member, IEEE) received the Laurea degree in biological science and the Ph.D. degree in experimental medicine from the Sapienza University of Rome, Rome, Italy, in 1987 and 1992, respectively.

Since 2005, she has been an Associate Professor of General Pathology with the Sapienza University of Rome. Her research interests are mainly focused on the study of the cytoskeletal actin organization, the process of invasiveness, and the formation of metastases of cultured cancer cells. In recent years, her scientific interest has been oriented toward the in vitro study of the effects of graphene-based nanomaterials on cultured cells. Her scientific activity is documented by 65 publications in international journals.

Daniela Uccelletti received the Laurea degree in biological science and the Ph.D. degree in cellular and developmental biology from the Sapienza University of Rome, Rome, Italy, in 1995 and 1999, respectively.

Since 2012, she has been an Associate Professor of Chemistry and Biotechnology of Fermentation with the Department of Biology and Biotechnologies, Sapienza University of Rome. She is a Steering Committee Member with the Research Center on Nanotechnology Applied to Engineering of Sapienza (CNIS) and the NMR-based Metabolomics Laboratory of Sapienza (NMLab), Sapienza University of Rome. She has coauthored three patents in the field of nanotechnologies. Her scientific activity is documented by 80 publications in international journals with referees and by participation in several national and international meetings. Her research interests are focused on the different fields of microbial biotechnology and the use of the *C. elegans* nematode as a model for toxicological studies and in relation to the processes involved in host–microorganism interactions. In recent years, her research has also been oriented to the field of nanotechnologies.

Maria Sabrina Sarto (Fellow, IEEE) received the Laurea (summa cum laude) and Ph.D. degrees in electrical engineering from the University of Rome "Sapienza," Rome, Italy, in 1992 and 1997, respectively.

From 2006 to 2015, she was the Director of the Research Center on Nanotechnology Applied to Engineering of Sapienza from 2006 to 2015, the Nanotechnology and Nanoscience Laboratory from 2010 to 2015, the Electromagnetic Compatibility Laboratory, Department of Electrical Engineering, since 1998, and the Department of Astronautical, Electrical and Energy Engineering, Sapienza University of Rome, since 2016; and the Deputy Rector of Research Infrastructures and Tools from 2014 to 2020. She has been a Full Professor of Electrotechnics and Electromagnetic Compatibility with the Faculty of Engineering, Sapienza University of Rome, since 2005, and the Deputy Rector of Research since 2020. She has authored or coauthored more than 210 articles in the field of electromagnetic compatibility (EMC), advanced materials for EMC, graphene-based materials for electromagnetic (EM) shielding and absorption, and sensing.

Prof. Sarto is a member of the Advisory Board of the IEEE Council on Nanotechnology. She was a recipient of several awards from the IEEE EMC Society and the Society of Automotive Engineers. She was a Distinguished Lecturer of the IEEE Electromagnetic Compatibility Society from 2001 to 2002. She was an Associate Editor of IEEE TRANSACTIONS ON ELECTROMAGNETIC COMPATIBILITY from 1998 to 2018, the Co-Chair of the IEEE Electromagnetic Compatibility Society TC11 on "Nanotechnology and Advanced Materials," the Chair of the working group IEEE Standard 299.1 of IEEE EMC Society, and the Co-Chair of the 2015 IEEE International Conference on Nanotechnology and EMC Europe 2020.

Open Access funding provided by 'Università degli Studi di Roma "La Sapienza" 2' within the CRUI CARE Agreement